Results and discussion of objective 2

Objective 2: Characterization and application of PAni biocomposites (doped and undoped) for removal of toxic heavy metal from landfill leachate.

5.1. Characterization of PAni biocomposites (doped and undoped)

Polyaniline (PAni) is a versatile redox active conductive polymer known for its excellent adsorption properties, making it a promising candidate for environmental remediation applications. In this study, two types of PAni-based bio-composites were synthesized by incorporating sugar cane bagasse and saw dust during synthesis, aiming to enhance the adsorption efficiency for metal ions. The bio-composites were prepared via a facile synthesis method and characterized using various physicochemical characterisation techniques including Fourier-transform infrared spectroscopy (FTIR), scanning electron microscopy (SEM), X-ray diffraction spectroscopy (XRD), Transmission electron microscopy (TEM), Energy dispersion x-ray spectroscopy (EDX).

5.1.1. Surface morphology by Scanning electron Microscope and EDX spectroscopy:

The surface morphology of the PAni based biocomposite adsorbents both in doped and Undoped state were investigated by Scanning Electron Microscopy (Model: JSM 6390LV, JEOL, JAPAN) and Energy Dispersive X-ray analysis (Model: JSM 6390LV, JEOL, JAPAN) studies. For investigating the surface morphology, the PAni based biocomposite samples were filtered and the residue of biocomposites after centrifugation was taken in a Petri dish and dried in a laboratory oven for 24 h at 60 °C. For SEM analysis the samples were properly dehydrated at 80 °C in an oven for 12 h. SEM and EDX analysis were done to investigate the characteristics of biosorbent (Siqueira et al., 2020). In order to understand the morphology of adsorbents on the biocomposites, SEM analyses of sugar cane bagasse and sawdust study were carried out and are shown in Fig.. The SEM of the surface of biocomposites were recorded at a very high magnification at an accelerating voltage of 20kV. The EDX investigation spectra (Fig.6) of sugarcane bagasse and sawdust biocomposites indicates that the biocomposites contain mainly the elements carbon and oxygen. The figures confirm that all atoms corresponding to sugar cane bagasse and SD are present (C and O). Furthermore, no other impurity-related peaks were observed, demonstrating the purity of synthesized PAni sugar cane bagasse and PAni-SD biocomposites. SEM micrographs at 500 times magnification revealed a diverse range of pores. There are holes and caverns type apertures on the surface of the adsorbent in the case of PAni biocomposites made from sugarcane bagasse and sawdust, indicating increased surface area accessible for adsorption. Furthermore, the fraction of oxygen atoms rose, indicating that oxyanions formed a portion of the adsorbed metal (Li et al., 2014).

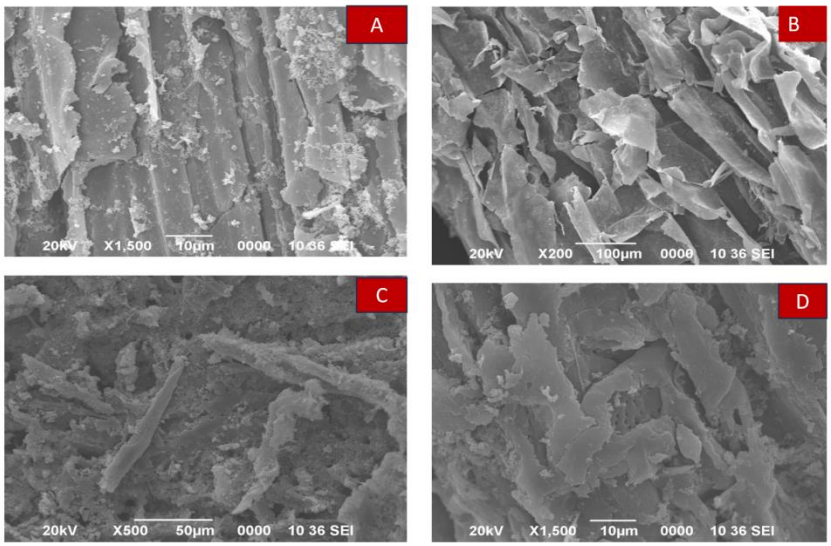

29

Fig.5.1. SEM micrographs of (A) PAni sugarcane bagasse (doped), (B) PAni sugarcane bagasse (undoped), (C) PAni SD (doped), (D)PAni SD (undoped) composite.

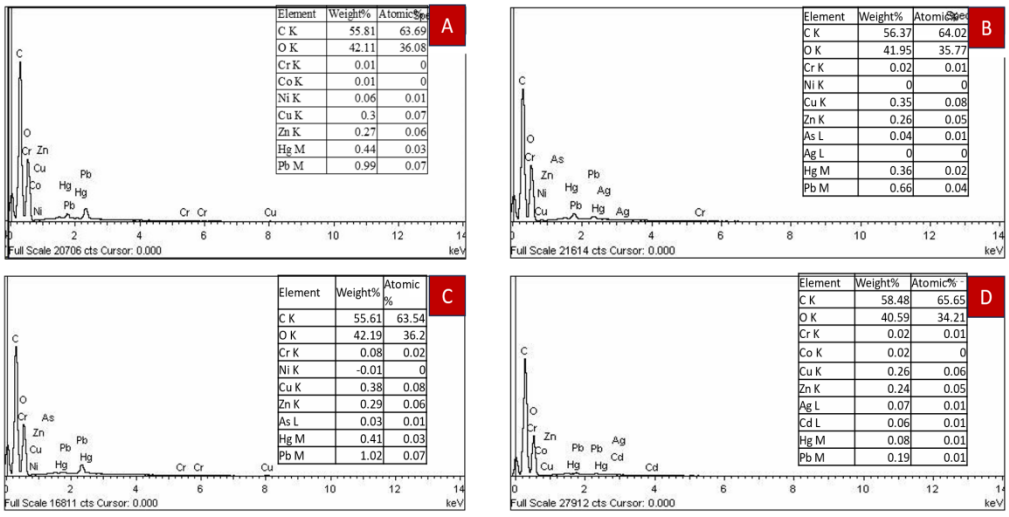

Fig.5.2. EDX spectroscopy of (A) PAni sugarcane bagasse (doped), (B) PAni sugarcane bagasse (undoped), (C) PAni SD (doped), (D)PAni SD (undoped) composite.

5.1.2. Transmission electron microscope for high resolution images:

Transmission electron microscopy (TEM) is an effective technique for observing the shape and size of particles at nanoscale resolution. TEM micrographs of polyaniline (PAni) using the TECNAI G2 20 S-TWIN (200KV) model from FEI Company, USA, are displayed in Figure 10. The PAni particles produced through oxidative aniline polymerization in an inorganic acid

aqueous solution exhibit high surface tension, leading to their tendency to aggregate and form large aggregates up to several microns. The primary units formed during the oxidative chemical polymerization of PAni are nanofibers, as also visible in SEM images (Figures 5.1.). As polymerization progresses, these nanofibers act as scaffolds for further PAni growth, eventually developing into particle forms. This results in non-uniform granular aggregation of pristine PAni due to irregular secondary growth. Nonetheless, TEM revealed smaller particles with compact biocomposite structures and fiber-like geometries, indicating a degree of fused surface and confirming the material's nanoscale characteristics.

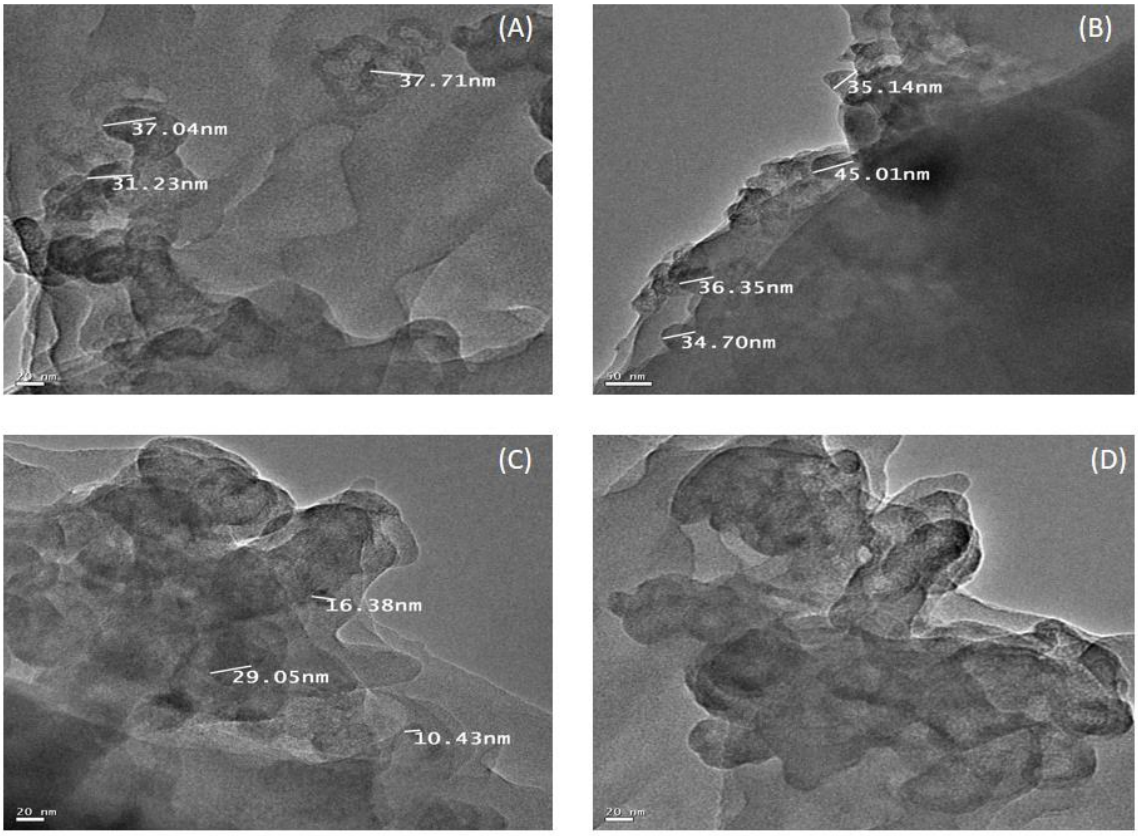

Fig.5.3. TEM micrographs of (A) PAni sugarcane bagasse (doped), (B) PAni sugarcane bagasse (undoped), (C) PAni SD (doped), (D)PAni SD (undoped) composite.

5.1.3. Chemical structure using FTIR

The structural characteristics of polyaniline (PAni) combined with sugarcane bagasse and PAni SD were analyzed using Fourier-transform infrared (FTIR) spectroscopy with models SPECTRUM 100 and FORNTIER IR from Perkin Elmer. The FTIR spectra, presented in Figure 5.4, revealed various functional groups present in the samples. A strong broad band in the 1405-1445 cm^{-1} region indicated the presence of alkanes group stretching vibrations. Peaks corresponding to the C–O deformation vibration were observed at 1382-1036 cm^{-1}. The absorption spectra exhibited a strong band at 1459-1591 cm^{-1}, signifying the presence of phenol rings. Additionally, the presence of hydrocarbons (C-H compounds) was evidenced by bands at 858-733 cm^{-1}. A peak at 1584 cm^{-1} also indicated the presence of phenol rings, while

the band at 1394 cm^{-1} represented the C–O bond. An absorption band at 1539 cm^{-1} confirmed another phenol ring, and the band at 1405-1445 cm^{-1} was attributed to alkanes. A dominant band at 1270-1150 cm^{-1} suggested the presence of ester carbonyl compounds, and the band at 1020-1220 cm^{-1} indicated C–N stretching in alkyl amines. Significant changes in the functional groups were recorded after subjecting the sample to these analyses, highlighting alterations in the chemical structure of PAni when combined with sugarcane bagasse and PAni SD.

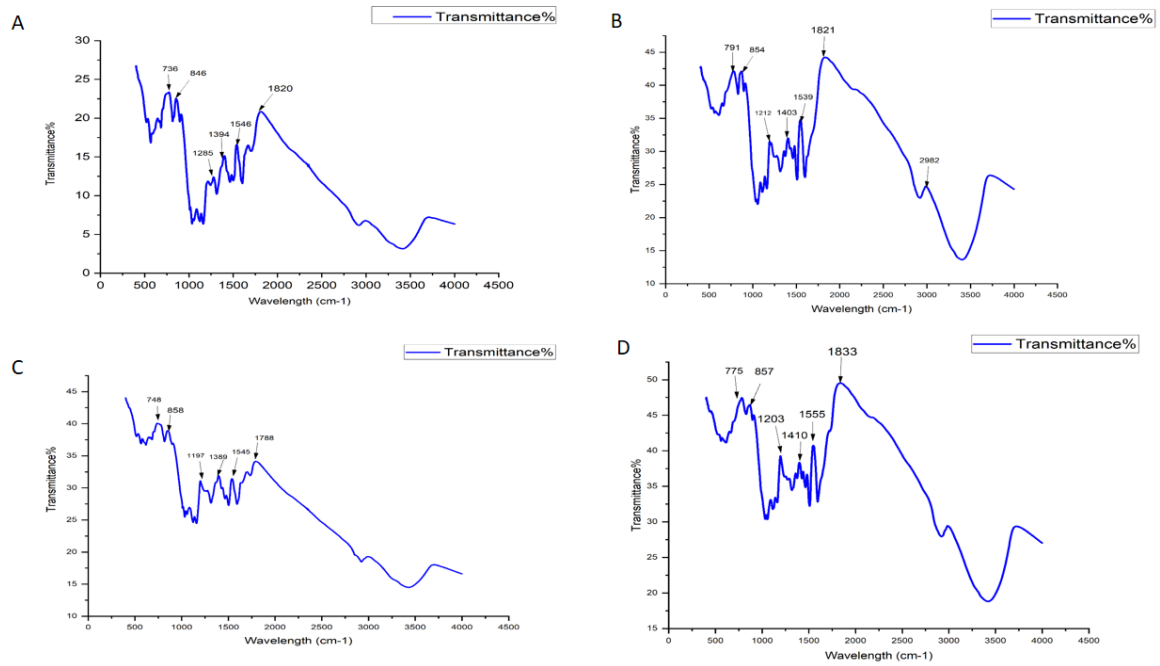

Fig.5.4. FTIR spectra of PAni biocomposites containing (A) sugarcane bagasse (doped), (B) sugarcane bagasse (undoped), (C) saw dust (doped) and (D) saw dust (undoped)

5.1.4. Physical structure using XRD:

The X-ray diffraction (XRD) patterns of nanocellulose-based composite films, analyzed using D8 FOCUS and MINIFIEX models from BRUKER AXS, Germany, and Rigaku Corporation, Japan, are presented in Figure 11. The diffraction peaks observed are characteristic of cellulose I, showing the highest intensity at a 2 theta angle of 22.5˚, with two additional weak peaks in the 2 theta regions of 14.6˚ and 16.4˚. Notably, no characteristic peaks for polyaniline (PAni) at 2 theta = 25˚ are observed, indicating a low crystalline level and content of PAni in the nanocellulose composite. This absence contrasts with the distinct crystalline structures seen in polyaniline/iron oxide and polyaniline/carbon nanotube nanocomposites, which typically exhibit clearer PAni peaks. The underlying reasons for the low crystallinity of PAni when formed on nanocellulose are not fully understood. It may be due to the interaction between PAni and the nanocellulose matrix, which could disrupt PAni's typical crystalline arrangement. Moreover, the analysis indicates that varying the content of PAni within the biocomposites does not significantly affect the XRD patterns, suggesting that the structural influence of PAni remains minimal regardless of its concentration in the composite films. This finding underscores the need for further investigation to understand the interactions at the molecular level that contribute to the observed low crystallinity of PAni in these nanocellulose-based composites.

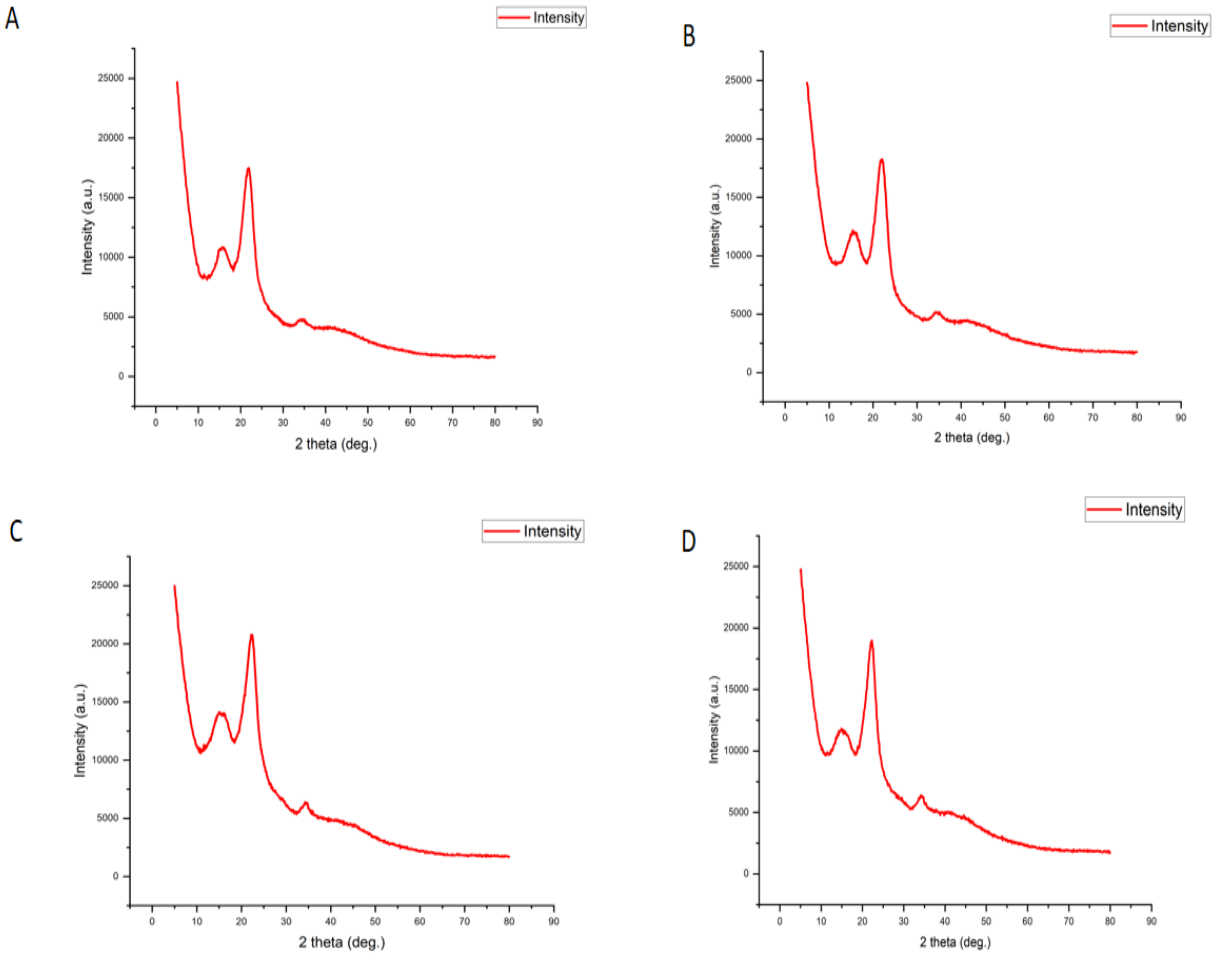

Fig.5.5. XRD patterns of PAni biocomposites containing (A) sugarcane bagasse (doped), (B) sugarcane bagasse (undoped), (C) saw dust (doped) and (D) saw dust (undoped)

5.2. Application of PAni biocomposites (doped and undoped) for removal of toxic heavy metal from landfill leachate:

After adsorption of heavy metals, changes in the morphology of the PAni biocomposites.

5.2.1. Scanning electron Microscope

The surface morphology of the prepared biocomposite adsorbent was completed by Scanning Electron Microscopy (SEM) and Energy Dispersive X-ray analysis (EDX) studies. The surface morphology of the biocomposites of sugar cane bagasse and SD both in doped and undoped state before and after treating the leachate were studied by SEM (Model: JSM-6390LV, designed by JEOL, Japan). For investigating the surface morphology, the leachate samples were filtered and the residue of biocomposites after centrifugation was taken in a Petri dish and dried in a laboratory oven for 24 h at 60ºC. The composites were then ground for 5- 10 mins with mortar and pastel to minute particles and these are analysed by EDX. For SEM analysis

the samples were properly dehydrated at 80ºC in an oven for 12 h. SEM and EDX analysis were done to investigate the characteristics of biosorbent (Siqueira et al., 2020).

5.2.2. Surface morphology and EDX spectroscopy:

In order to understand the morphology of adsorbents on the biocomposites, SEM analyses of sugar cane bagasse and sawdust before and after adsorption study were carried out and are shown in Fig. 5.8 and Fig. 5.9 respectively. The SEM of the surface of biocomposites were recorded at a very high magnification at an accelerating voltage of 20kV. EDX analysis of the as-prepared, PAni-SD both in doped and undoped state, and PAni sugar cane bagasse both in doped and undoped state, after treatment with toxic metal-containing leachate adsorption study were carried out and the outcomes are reported in Fig. 5.6.and Fig. 5.7. The EDX investigation spectra (Fig.5.6 and Fig.5,7) of untreated sugarcane bagasse and sawdust biocomposites indicates that the biocomposites contain chiefly the elements carbon and oxygen. The figures confirm that all atoms corresponding to sugar cane bagasse and SD are present (C and O). Furthermore, no other impurity-related peaks were observed, demonstrating the purity of synthesized PAni sugar cane bagasse and PAni -SD biocomposites. The comparison of SEM images of the before and after adsorption shows that there are morphological changes in the surface of the biocomposite samples after adsorption. It is observed that the bubble-like structures are surrounded by the surface of the biocomposites. The precipitates and complexes formed by the heavy metal ions can also be observed. Smooth markings may be seen on the surface in the images. SEM micrographs of activated carbon at 500 times magnification revealed a diverse range of pores. There are holes and caverns type apertures on the surface of the adsorbent in the case of PAni biocomposites made from sugarcane bagasse and sawdust, indicating that there is increased surface area accessible for adsorption. The EDX data of PAni sugar cane bagasse and PAni SD biocomposites, after the adsorption of toxic metals study reveal the presence of additional peaks. The adsorption of hazardous metal ions is confirmed from these peaks as can be observed in figure 6 (Karthik and Meenakshi 2014). Furthermore, the fraction of oxygen atoms rose, indicating that oxyanions formed a portion of the adsorbed metal (Li et al., 2014). After the adsorption of toxic metals on the PAni -sugar cane and PAni-SD the metal concentration were decreased in the leachate. These changes were expected as a result of the adsorption of toxic metals. The EDX analysis shows increased the peaks in PAni biocomposites after treatment.

The elemental mapping analysis of PAni sugar cane bagasse and PAni-SD is presented in fig.5.6 and fig. 5.7 respectively. The achieved micrographs display the distribution of the principal constituents of PAni- sugar cane bagasse and PAni-SD biocomposites. The distribution of toxic metals on the PAni -sugar cane bagasse and PAni-SD surface confirms its uptake on the adsorbent material.

The EDX images of before and after the adsorption process, revealed a change in the morphology of the adsorbent too. The EDX spectrum also supports the ICP-MS results of good metal adsorption by the biocomposites (Fig.5.6, Fig.5.7).

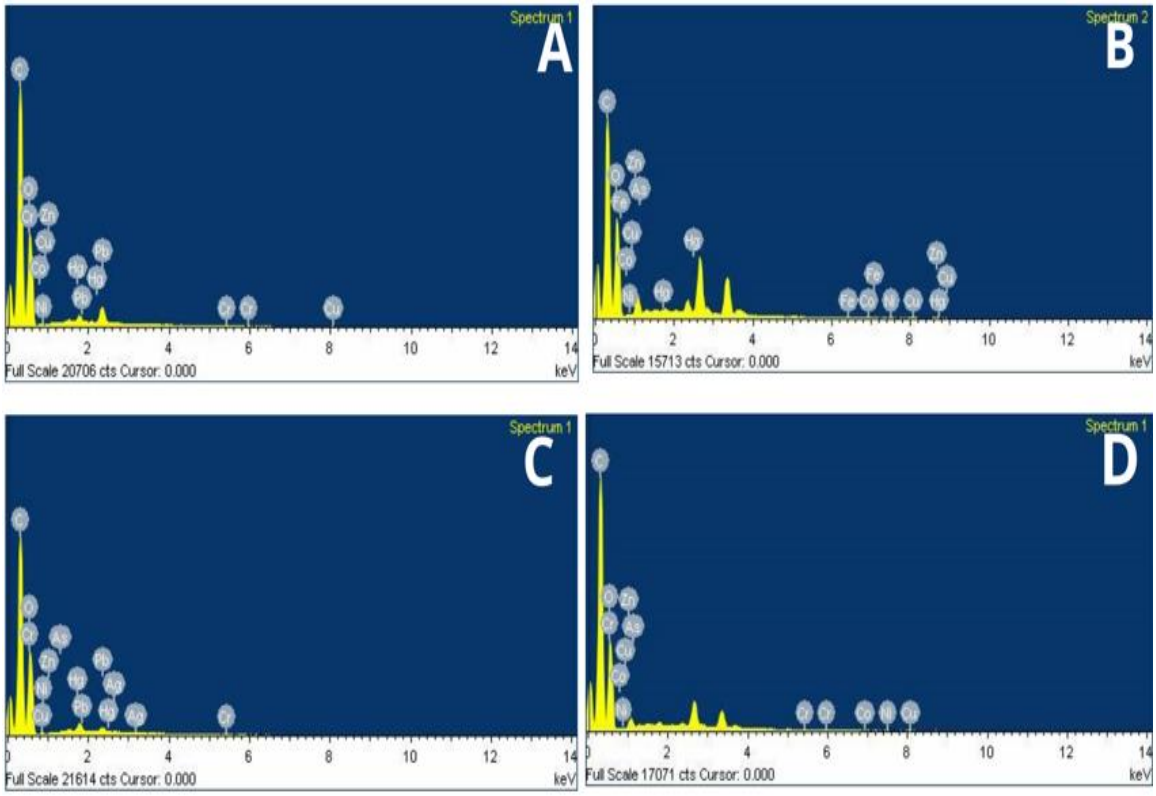

Fig.5.6. EDX Analyses for Sugar cane bagasse both treated and untreated nanoparticles. (A)Sugarcane (doped) before treatment; (B) Sugarcane (doped) after treatment ; (C) Sugarcane(undoped) before treatment; (D)Sugar cane (undoped) after treatment.

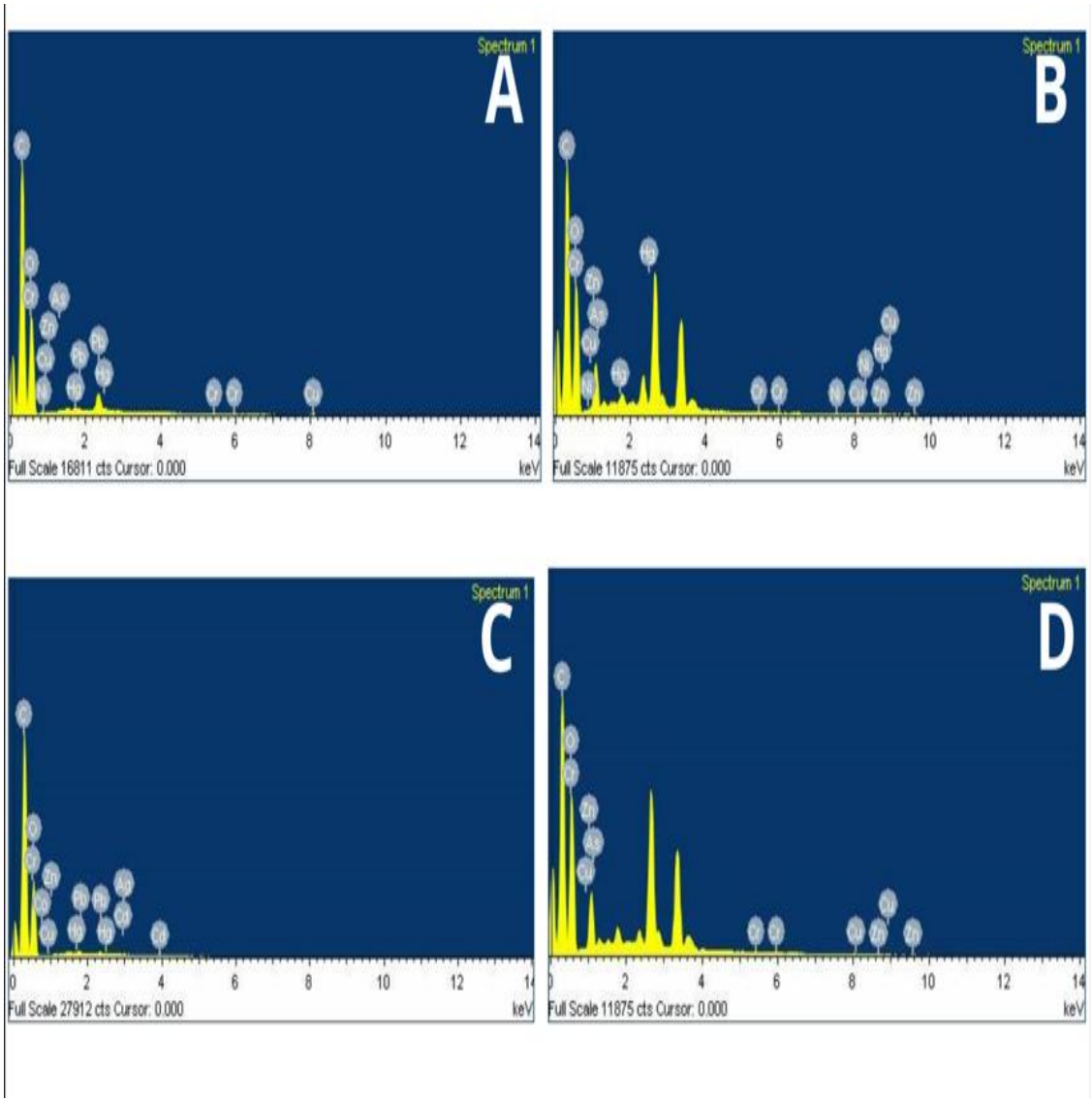

Fig. 5.7. EDX Analyses of Sawdust bagasse both treated and untreated nanoparticles. (A) Sawdust (doped) before treatment; (B) Sawdust (doped) after treatment; (C) Sawdust(undoped) before treatment; (D)Sawdust(undoped) after treatment.

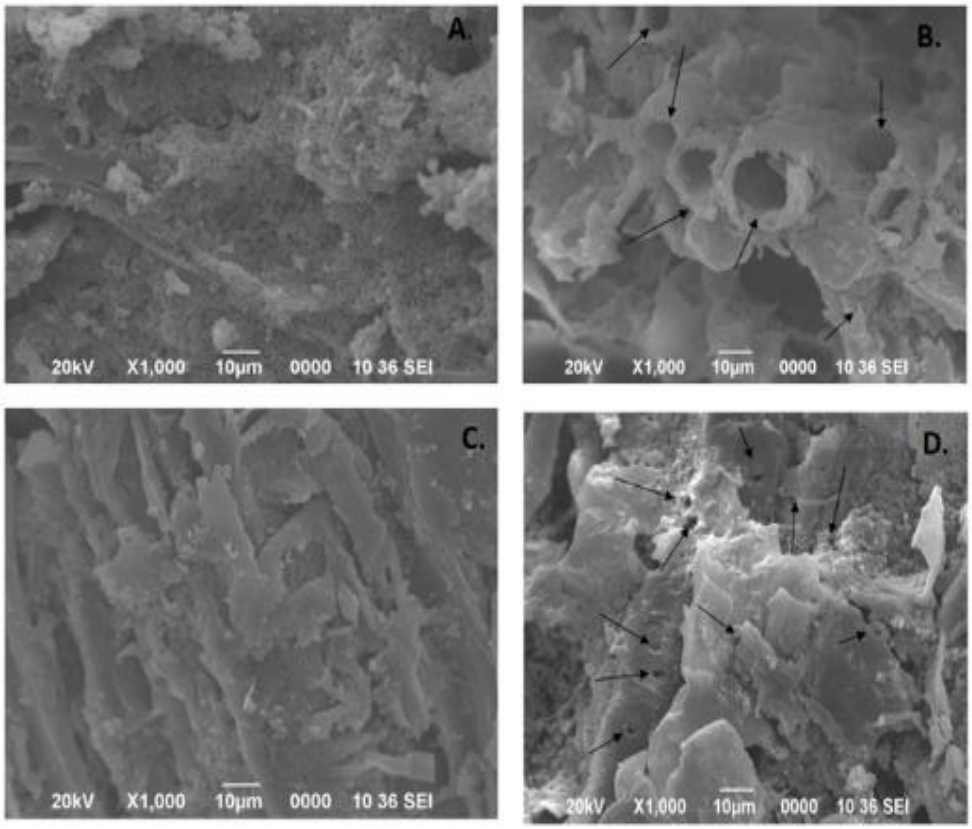

Fig.5.8. SEM images of the (A) Sugarcane (doped) before treatment; (B) Sugarcane bagasse (doped) after treatment;(C) Sugarcane bagasse(undoped) before treatment; (D)Sugar cane bagasse(undoped) after treatment.

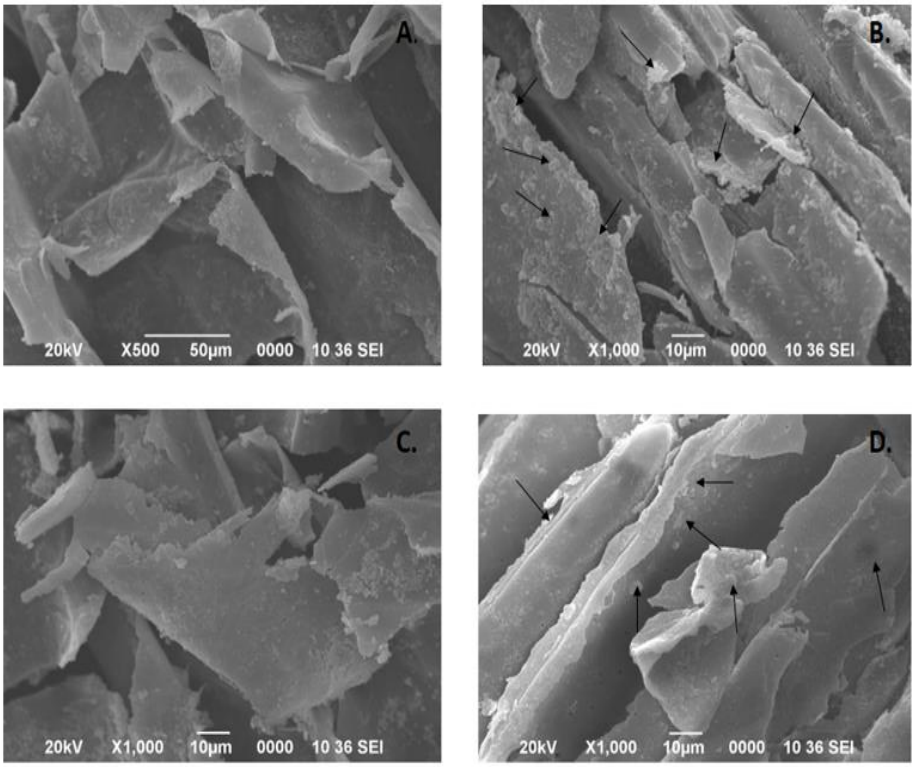

Fig. 5.9. SEM images of the (A)SD(doped)before treatment; (B) SD(doped) after treatment;(C) SD(un doped) before treatment; (D)SD(un doped) after treatment.

5.3. Adsorption study

The concentration of the eight toxic metals (B, Cr, Co, Ni, Zn, Ag, Cd, Pb), removed from leachate were observed from the Table 5.1. In Table 5.2, and the removal efficiency as well as adsorption capacity is calculated. The B removal efficiency is seen to be higher in PAni SD undoped bicomposite i.e, 75.59% and lower in sugarcane bagasse undoped biocomposites in the 24 h adsorption study. Similarly in case of Cr, higher removal efficiency was observed in case of PAni SD undoped i.e, 53.49% and lower in PAni sugar cane bagasse doped composite. Higher removal efficiency Co was observed in case of PAni SD doped i.e, 80.55% and lower in PAni sugar cane bagasse doped composite. On the other hand, in case of Ni and Zn, removal efficiency is higher in PAni SD doped i.e, 67.89% and 38.3% respectively and lower in PAni-sugarcane undoped biocomposite. The removal efficiency of Ag, Cd, and Pb is higher in PAni SD doped which is 97.09%, 80.3% and 74.25% respectively. So, it can be inferred that PAni-SD both doped and undoped was found to be more efficient in removing HMs from leachate.

Table.5.1. Metal removal efficiency of different biocomposites sugar cane bagasse and saw dust adsorbent.

S. No	Metal removal efficiency	sample Sites	Sawdust(doped)%	Saw dust (Un doped)%	Sugar cane(Un doped)%	Sugar cane(Un doped)%
1		site-1	70.90±0.64	73.45±0.9	70.54±0.88	68.32±0.67
2		site-2	66.48±0.54	72.58±0.89	68.6±0.83	63.64±0.83
3		site-3	73.34±0.40	73.57±0.85	67.56±1.48	37.23±0.8
4		site-4	84.84±3.20	80.66±0.76	68.9±0.95	75.37±0.86
5	Boron	site-5	80.96±0.65	77.73±0.73	66.71±0.74	69.27±0.59
6		site-1	47.88±2.89	57.58±1.05	56.95±1.35	53.89±0.7
7		site-2	BDL	22.84±0.69	37.71±0.71	36.7±0.81
8		site-3	83.61±1.43	75.78±0.71	43.98±1.35	56.51±0.75
9		site-4	71.02±0.71	48.37±0.53	53.88±1.19	48.47±0.53
10	Chromium	site-5	65.95±0.99	63.56±0.47	58.22±0.76	60.84±0.79
11		site-1	73.94±0.41	73.34±0.7	74.51±0.63	71.01±0.89
12		site-2	84.85±0.75	64.58±0.66	67.71±0.84	64.39±0.68
13		site-3	84.89±0.6	83.59±0.62	20.83±1.09	82.68±0.58
14		site-4	81.24±0.39	70.17±1.11	74.21±0.78	68.57±0.92
15	Cobalt	site-5	77.91±0.81	74.48±0.55	75.40±0.82	74.28±0.75
16		site-1	70.14±0.73	69.4±0.97	71.3±0.91	68.48±0.88
17		site-2	47.68±2.2	50.44±1.14	51.73±0.99	51.8±0.81
18		site-3	83.24±2.79	77.14±0.71	85.52±0.91	62.55±1.06
19		site-4	74.99±1.17	57.55±1.08	57.59±0.85	53.43±0.52
20	Nickel	site-5	66.16±1.54	68.25±0.86	69.43±0.62	69.55±0.77
21		site-1	**BDL**	**BDL**	**BDL**	4.71±0
22		site-2	37.40±1.88	50.91±1.16	15.09±0.91	37.73±0.77
23		site-3	74.21±2.1	68.57±0.83	99.29±0.53	99.5±0.5
24		site-4	58.46±1.15	46.81±0.72	35.25±0.99	24.74±0
25	Zinc	site-5	46.81±0.78	26.74±0.77	27.65±0.73	21.55±2.44
26		site-1	94.63±0.88	97.49±0.88	97.41±0.67	98.45±0.77
27		site-2	98.53±0.86	91.28±0.8	97.10±0.78	97.59±0.69
28		site-3	97.79±0.76	**BDL**	97.54±0.97	98.52±0.83
29		site-4	96.12±1.81	97.8±1.1	98.70±0.75	98.63±0.72
30	Silver	site-5	97.08±2	34.38±0.66	89.71±0.71	97.28±0.67
31		site-1	85.75±0.81	88.96±1.08	85.66±0.46	89.63±0.72
32		site-2	99.33±0.78	74.19±0.91	69.61±0.66	62.73±0.8
33		site-3	74.12±0.45	76.71±0.58	99.09±0.56	99.06±0.86
34	Cadmium	site-4	79.58±0.85	62.67±1.52	68.51±0.46	34.19±0.73

35		site-5	64.01±0.65	71.51±1.07	59.50±0.93	78.68±0.52
36		site-1	22.72±0.89	40.57±1.01	31.22±0.97	37.74±0.55
37		site-2	99.17±0.7	64.57±0.83	40.7±0.93	17.61±0.78
38		site-3	98.39±0.52	97.49±0.89	99.78±0.23	99.24±0.58
39		site-4	81.69±1.54	72.76±0.8	49.77±0.66	66.77±0.71
40	Lead	site-5	69.49±0.56	71.90±0.74	69.71±0.77	55.82±0.74

Table.5.2. The adsorption capacity of different biocomposites sugar cane bagasse and sawdust adsorbent.

S. No	Adsorption capacity	sample Sites	Sawdust (doped)	Sawdust (Undoped)	Sugarcane (doped)	Sugarcane (Undoped)
			17.31±0.16			
1	Boron	site-1		17.6±0.2	17.38±0.06	16.75±0.25
2		site-2	12.47±0.34	14.4±0.3	13.33±0.14	12.17±0.02
3		site-3	17.6±0.31	17.3±0.3	16.36±0.26	9.08±0.07
4		site-4	12.54±0.17	12.4±0.2	10.30±0.26	11.40±0.29
5		site-5	23.34±0.41	22.5±0.1	19.25±0.15	19.60±0.24
6	Chromium	site-1	1.59±0.28	30.2±0.1	1.49±0.27	1.56±0.17
7		site-2	-	0.0	0.44±0.03	0.45±0.06
8		site-3	2.84±0.15	73.7±0.3	1.52±0.07	2.53±0.49
9		site-4	0.77±0.04	19.3±0.3	0.55±0.04	0.61±0.22
10		site-5	2.81±0.07	68.4±0.2	2.48±0.02	2.64±0.17
11	Cobalt	site-1	1.74±0.24	1.8±0.1	1.68±0.22	1.85±0.02
12		site-2	2.05±0.02	1.5±0.3	1.68±0.19	1.68±0.17
13		site-3	2.16±0.18	2.4±0.3	0.5±0.04	1.86±0.12
14		site-4	1.73±0.20	1.4±0.1	1.62±0.08	1.42±0.06
15		site-5	2.16±0.3	1.7±0.2	1.93±0.05	1.96±0.01
16	Nickel	site-1	3.46±0.31	3.8±0.1	3.81±0.11	3.75±0.05
17		site-2	1.85±0.16	2.4±0.3	2.18±0.08	2.23±0.19
18		site-3	4.56±0.2	4.5±0.3	4.5±0.27	3.57±0.05
19		site-4	2.56±0.21	1.8±0.2	1.69±0.23	1.75±0.03
20		site-5	4.77±0.23	4.8±0.1	4.8±0.09	4.82±0.08
21	Zinc	site-1	-	-	-	0.17±0.02
22		site-2	1.62±0.22	1.7±0.3	0.49±0.15	1.42±0.02
23		site-3	4.33±0.23	4.3±0.3	5.8±0.09	5.84±0.03
24		site-4	1.19±0.09	0.8±0.2	0.65±0.04	0.45±0.03
25		site-5	1.49±0.16	1.0±0	0.92±0.07	0.75±0.02
26	Silver	site-1	1.45±0.09	1.6±0.3	1.57±0.07	1.54±0.04
27		site-2	1.52±0.25	1.5±0.2	1.68±0.02	1.65±0.11
28		site-3	0.2±0.11	-	0.16±0.02	0.16±0.03
29		site-4	0.78±0.07	0.5±0.2	0.79±0.03	0.75±0.03
30		site-5	1.35±0.41	0.4±0.2	0.96±0.01	1.04±0.01
31	Cadmium	site-1	0.04±0.02	0.1±0	0.05±0.01	0.04±0.01
32		site-2	0.03±0.01	0.0	0.02±0.01	0.02±0.02
33		site-3	0.03±0.01	0.0	0.03±0.02	0.03±0.01
34		site-4	0.00	0.0	0.00	0.00
35		site-5	0.02±0.01	0.0	0.02±0.01	0.01±0.01
36	Lead	site-1	0.03±0.01	0.1±0	0.07±0.01	0.08±0.01
37		site-2	0.4±0.18	0.3±0.2	0.17±0.01	0.07±0.01
38		site-3	0.84±0.021	0.8±0	0.84±0.03	0.85±0.01
39		site-4	0.06±0.02	0.1±0	0.05±0.02	0.07±0.02
40		site-5	0.26±0.02	0.3±0.2	0.23±0.01	0.19±0.02

5.4. Summary of this chapter:

The chapter details the development and evaluation of novel polyaniline (PAni)-based biocomposites synthesized through the polymerization of aniline on the surfaces of sugarcane bagasse and sawdust. Para toluene sulfonic acid was used as a dopant to enhance the adsorption properties and surface chemistry of the PAni composites. Various characterization techniques, including SEM, EDX, TEM, FT-IR, and XRD, were employed to analyze the surface characteristics of the composites. These hybrid materials were subsequently utilized as cost-effective adsorbents for removing toxic metals from leachate solutions at a dumping site.

The synthesis involved in situ polymerization of aniline in the presence of sugarcane bagasse and sawdust, which were then ground to nanoscale particles. The maximum removal efficiencies for various metals were determined, with the undoped PAni-sawdust (PAni-SD) biocomposite showing the highest removal rates for boron (75.59%) and chromium (53.49%). For other metals like cobalt, nickel, zinc, silver, cadmium, and lead, the doped PAni-sawdust biocomposites exhibited the highest removal efficiencies, reaching up to 97.09% for silver.

The study concludes that undoped PAni-SD biocomposites are particularly effective in removing toxic metals from leachate and outperform other adsorbents cited in the literature. These findings suggest that PAni-biocomposites are environmentally friendly and affordable bioadsorbents suitable for heavy metal remediation in landfill leachates. Future research will focus on improving the adsorption capacities and regenerating the biocomposites for repeated use, reinforcing their potential as practical adsorbents for treating toxic metal-contaminated wastewater. Overall, the chapter highlights the promising application of PAni biocomposites in environmental cleanup efforts.

References:

1. Siqueira T C A, da Silva I Z, Rubio A J, Bergamasco R, Gasparotto F, Paccola E A de S, Yamaguchi N U (2020). Sugarcane bagasse as an efficient biosorbent for methylene blue removal: Kinetics, isotherms and thermodynamics. International Journal of Environmental Research and Public Health, 17(2). https://doi.org/10.3390/ijerph17020526